AIP Applied Physics Letters

Effects of microwave annealing on electrical enhancement of amorphous oxide semiconductor thin film transistor

Li-Feng Teng, Po-Tsun Liu, Yuan-Jou Lo, and Yao-Jen Lee

Citation: Applied Physics Letters **101**, 132901 (2012); doi: 10.1063/1.4754627
View online: http://dx.doi.org/10.1063/1.4754627
View Table of Contents: http://scitation.aip.org/content/aip/journal/apl/101/13?ver=pdfcov
Published by the AIP Publishing

Articles you may be interested in
Coplanar amorphous-indium-gallium-zinc-oxide thin film transistor with He plasma treated heavily doped layer
Appl. Phys. Lett. **104**, 022115 (2014); 10.1063/1.4862320

Effect of annealing time on bias stress and light-induced instabilities in amorphous indium–gallium–zinc-oxide thin-film transistors
J. Appl. Phys. **110**, 114503 (2011); 10.1063/1.3662869

Trap-limited and percolation conduction mechanisms in amorphous oxide semiconductor thin film transistors
Appl. Phys. Lett. **98**, 203508 (2011); 10.1063/1.3589371

Correlation of photoconductivity response of amorphous In–Ga–Zn–O films with transistor performance using microwave photoconductivity decay method
Appl. Phys. Lett. **98**, 102107 (2011); 10.1063/1.3561755

Role of order and disorder on the electronic performances of oxide semiconductor thin film transistors
J. Appl. Phys. **101**, 044505 (2007); 10.1063/1.2495754

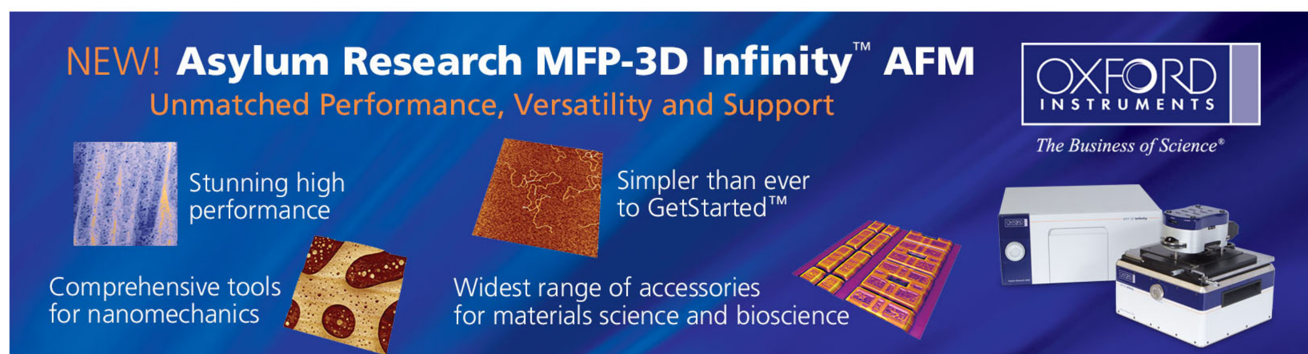

This article is copyrighted as indicated in the article. Reuse of AIP content is subject to the terms at: http://scitation.aip.org/termsconditions. Downloaded to IP: 140.113.38.11 On: Thu, 01 May 2014 08:31:59

Effects of microwave annealing on electrical enhancement of amorphous oxide semiconductor thin film transistor

Li-Feng Teng,[1] Po-Tsun Liu,[2,a)] Yuan-Jou Lo,[3] and Yao-Jen Lee[4]
[1]*Department of Photonics and Institute of Electro-Optical Engineering, National Chiao Tung University, Hsinchu 30010, Taiwan*
[2]*Department of Photonics and Display Institute, National Chiao Tung University, HsinChu 30010, Taiwan*
[3]*College of Photonics and Institute of Photonic System, National Chiao Tung University, Tainan City 71150, Taiwan*
[4]*National Nano Device Laboratories, Hsinchu 30078, Taiwan*

(Received 13 August 2012; accepted 10 September 2012; published online 24 September 2012)

By using microwave annealing technology instead of thermal furnace annealing, this work elucidates the electrical characteristics of amorphous InGaZnO thin film transistor (a-IGZO TFT) with a carrier mobility of 13.5 cm^2/Vs, threshold voltage of 3.28 V, and subthreshold swing of 0.43 V/decade. This TFT performance with microwave annealing of 100 s is well competitive with its counterpart with furnace annealing at 450 °C for 1 h. A physical mechanism for the electrical improvement is also deduced. Owing to its low thermal budget and selective heating to materials of interest, microwave annealing is highly promising for amorphous oxide in semiconductor TFT manufacturing. © *2012 American Institute of Physics*. [http://dx.doi.org/10.1063/1.4754627]

Owing to their high carrier mobility, transparency for visible light, high process compatibility with present solid-state semiconductor technologies, and available room-temperature deposition, transparent amorphous InGaZnO thin films have received considerable attention for their use in next-generation active-matrix liquid-crystal display (AMLCD) and organic light-emitting diode display (AMOLED) technologies.[1–5] Sputter deposition technology is widely adopted, especially for the large-size amorphous InGaZnO thin film transistor (a-IGZO TFT) display backplane manufacturing. The sputter-deposited a-IGZO active layer typically requires thermal annealing at around 400 °C for 30 min or longer to achieve a satisfactory device performance and stability.[6–8] For conventional furnace annealing, thermal energy is transferred to the material of interest by creating a temperature gradient from outward to inward, resulting in additional thermal energy consumption. However, furnace annealing is limited by low efficiency of heating and high thermal budget process. This work presents a novel microwave annealing process for a-IGZO TFT fabrication with low thermal budget process. Microwave heating process can transfer the energy directly to the target materials by absorption of microwave energy throughout the volume of the material. Among its advantages include thermal uniformity, rapid heating process, shortened manufacturing period, low thermal budget, and suppression of unexpected species diffusion.[9] Microwave heating is also characterized by selective heating of materials, which is impossible with the typical furnace annealing process.[10,11] This work also investigates how microwave annealing affects the electrical performance and reliability of a-IGZO TFTs. A physical mechanism responsible for the electrical enhancement of a-IGZO TFT is also proposed by comparing with the counterpart of a-IGZO TFT thermally annealed in a typical furnace at 450 °C for 1 h.

TFT devices with an inverted staggered bottom gate structure without backchannel passivation were fabricated on a glass substrate. A 100-nm-thick Mo layer was formed as a bottom gate electrode in a DC sputtering system, followed by the subsequent deposition of a 150-nm-thick silicon nitride (SiN_x) on the patterned gate electrode by plasma-enhanced chemical vapor deposition (PECVD). Next, the active channel layer of a 50-nm-thick a-IGZO layer was formed by DC sputtering at a power of 100 W with an argon flow rate of 10 sccm at room temperature. The target for the a-IGZO film deposition was an IGZO pellet with the component ratio of 1:1:1:4 at. % (In:Ga:Zn:O). A 100-nm-thick indium tin oxide (ITO) was then formed to act as source/drain electrodes by RF sputtering; all of the layers were defined by the shadow masks. The channel width and length of a-IGZO TFTs were varied from 200 to 1000 μm. All samples were annealed sequentially in a microwave annealing system with a microwave frequency of 5.8 GHz,[12] as shown in Fig. 1(a). The microwave power used in this work is 600 W and 1200 W, as denoted by 1P and 2P, respectively. Microwave annealing lasted from 100 s to 600 s. The absorption of electromagnetic wave energy is generally in the frequency range of 2 to 18 GHz for ZnO-based materials.[13,14] Therefore, as is expected, the a-IGZO active layer effectively absorbs the microwave energy with the frequency we used in this work. Additionally, a control sample of a-IGZO TFT with a typical thermal annealing process was fabricated for comparison with microwave annealed a-IGZO TFT. The thermal annealing was conducted in a furnace with N_2 gas flow rate of 10 l/h at 450 °C for 1 h. Electrical and reliability measurements were carried out using the semiconductor parameter analyzer, Keithley 4200. For the x-ray photoelectron spectroscopy (XPS) measurement, 50-nm a-IGZO thin films with various microwave annealing conditions were deposited separately on n-type Si wafer.

Figure 1(b) shows the transfer characteristics of a-IGZO TFTs with different microwave annealing conditions at a drain-to-source voltage (V_{DS}) of 11 V. The extracted threshold voltage (V_{th}) and mobility of each a-IGZO TFT were also

a)E-mail: ptliu@mail.nctu.edu.tw.

 © 2012 American Institute of Physics

This article is copyrighted as indicated in the article. Reuse of AIP content is subject to the terms at: http://scitation.aip.org/termsconditions. Downloaded to IP: 140.113.38.11 On: Thu, 01 May 2014 08:31:59

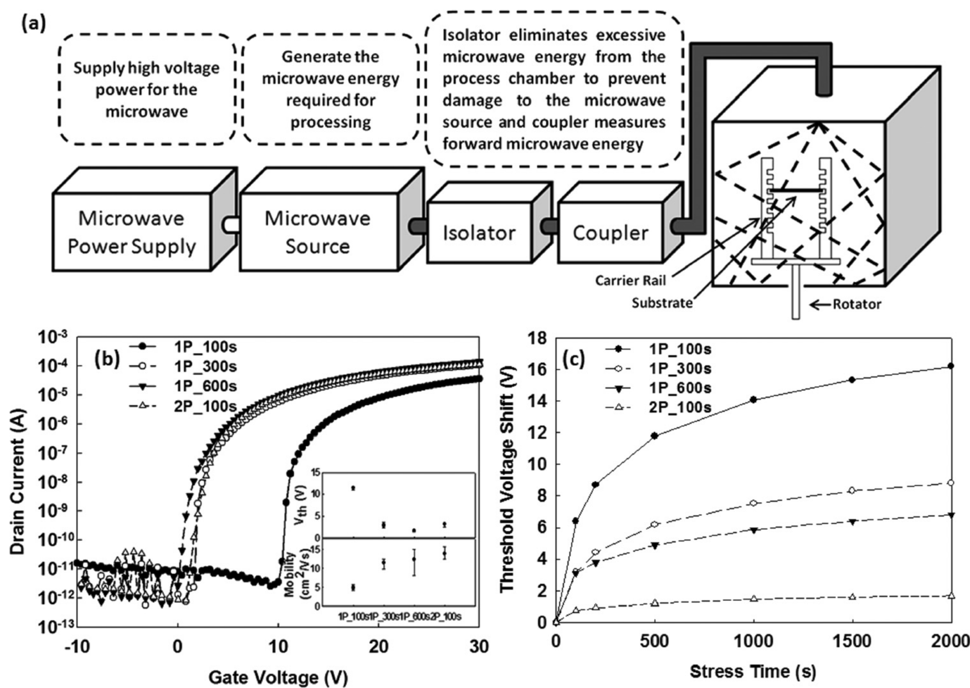

FIG. 1. (a) The schematic of microwave annealing system in this work. (b) The drain current (I_D) versus gate voltage (V_G) curves of a-IGZO TFTs with different microwave annealing processes, at a drain-to-source voltage (V_{DS}) of 11 V. The symbols of 1P_100s, 1P_300s, 1P_600s, and 2P_100s stand for the microwave annealed a-IGZO TFTs with 1P (600 W) for 100, 300, and 600 s, and 2P (1200 W) for 100 s, respectively. The corresponding device parameters, such as threshold voltage (V_{th}) and mobility of a-IGZO TFTs are shown in the inset. (c) Threshold voltage shift of microwave-annealed a-IGZO TFTs as a function of gate bias stress durations. The electric field of gate bias stress was fixed at 2.5 MV/cm. The V_{th} shift was defined as the difference of the threshold voltages before and after the gate bias stress application to the a-IGZO TFT device.

compared in the inset. According to this figure, the threshold voltage of a-IGZO TFT decreased from 11.4 to 1.62 V, as the microwave annealing duration increased from 100 s to 600 s, respectively, with an identical microwave power. Moreover, the mobility increased when increasing the microwave annealing time, indicating that increasing the microwave annealing time improved the electrical characteristics of a-IGZO TFTs. As microwave power increases from 1P to 2P with the same process time, the mobility of a-IGZO TFTs is enhanced significantly from 4.86 to 13.9 cm^2/Vs; in addition, the threshold voltage is lowered from 11.4 to 3.13 V.

This work also studied how gate bias stress (GBS) affects a-IGZO TFTs with different microwave annealing conditions, as shown in Fig. 1(c). In the gate bias stress measurements, an electric field of 2.5 MV/cm was applied to gate electrode and source/drain electrodes were grounded. This finding suggests that increasing both microwave power and treatment duration can improve the electrical reliability of a-IGZO TFT. The V_{th} shift of microwave annealed a-IGZO TFT after GBS testing was decreased from the value of 16.2 V with the condition of 1P power for 100 s to a minimum of 1.6 V with 2P power for 100 s. Also, increasing the microwave power and annealing duration can enhance microwave energy absorption capacity for the a-IGZO active layer. The material analysis method was performed further to observe the evolution of a-IGZO film structure, allowing us to identify the physical mechanism responsible for improving the electrical properties of a-IGZO TFT devices.

Figure 2 shows the XPS analysis results of O1s spectrum for the a-IGZO thin film with microwave annealing treatments. Two components of O1s peaks could be fitted by Gaussian Lorentzian deconvolution, which centered at 530.6 and 531.4 eV, respectively. The lower binding energy centered at 530.6 eV, denoted as peak A, originated from the lattice oxygen ions with neighboring metal atoms.[15,16] The higher binding energy peak at 531.4 eV, denoted as peak B, corresponds to O^{2-} ion at an oxygen-deficient region in the matrix of the a-IGZO film.[8,17] According to the results of XPS, peak A increased and peak B decreased while the microwave annealing duration increased, as shown in Figs. 2(a)–2(c), respectively. Also, the XPS spectrum of a-IGZO film with high-power microwave annealing was composed of a high intensity of peak A and low intensity of peak B, as shown in Fig. 2(d). This figure revealed a high content of lattice oxygen ions in the microwave-annealed a-IGZO films with few oxygen-deficient regions as the microwave power was increased. XPS analysis results confirmed that the microwave annealing process assisted the oxygen ions binding with metal atoms and suppressed the formation of oxygen-deficient region in the a-IGZO films when increasing both the microwave power and annealing duration.

Figure 3 compares the effects of microwave and typically used furnace annealing on a-IGZO TFT. The a-IGZO TFT with 2P microwave annealing for 100 s exhibited a superior performance with a higher mobility and lower subthreshold swing than that of the 450 °C furnace-annealed a-IGZO TFT as shown in the inset of Fig. 3(a). After GBS, the microwave annealed a-IGZO TFT also revealed a comparable reliability with the furnace-annealed one, as shown in Fig. 3. Trap densities (N_t) can be estimated from subthreshold swing value with the following formula:

$$S.S. = \log_e 10 \times k_B T/e[1 + e(tN_t + D_{it})/C_i], \quad (1)$$

where k_B denotes the Boltzmann constant; T represents the temperature; e is the elementary electric charge; t is the thickness of the a-IGZO active layer; and D_{it} is the interface trap density, assuming the trap tN_t dominated and D_{it} is negligible.[6] The N_t value of a-IGZO TFT with microwave and furnace annealing was 2.49×10^{17} and $3.51 \times 10^{17}\ cm^{-3}$, respectively. The microwave-annealed a-IGZO exhibited a lower trap density than that of the furnace-annealed one. Figure 3(b) shows the XPS O1s spectrum of a-IGZO thin film with 2P microwave annealing for 100 s and furnace

This article is copyrighted as indicated in the article. Reuse of AIP content is subject to the terms at: http://scitation.aip.org/termsconditions. Downloaded to IP: 140.113.38.11 On: Thu, 01 May 2014 08:31:59

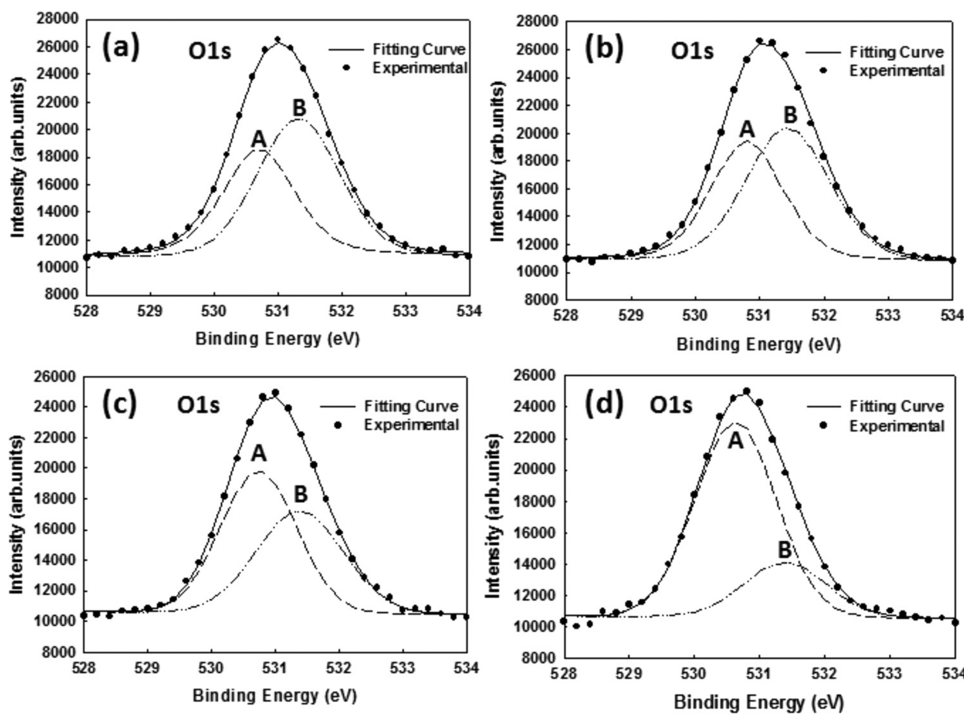

FIG. 2. XPS analyses of O1s spectrum for the a-IGZO films with microwave annealing at (a) 1P for 100 s, (b) 1P for 300 s, (c) 1P for 600 s, and (d) 2P for 100 s, respectively. Peak A denotes the lower binding energy peak centered at 530.6 eV, generated from the lattice oxygen ions with neighboring metal atoms. Peak B is the higher binding energy peak at 531.4 eV corresponding to O^{2-} ion at an oxygen-deficient region with the matrix of the a-IGZO film.

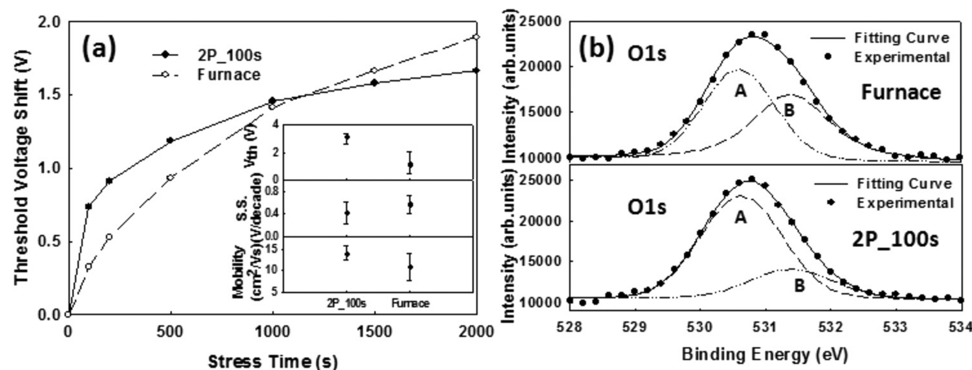

FIG. 3. (a) The comparison of threshold voltage shift between the a-IGZO TFT with microwave annealing at 2P for 100 s and furnace annealing at 450 °C for 1 h, as a function of gate bias stress durations. The electric field of gate bias stress was fixed at 2.5 MV/cm. The inset shows threshold voltage (V_{th}), subthreshold swing (S.S), and mobility of the fresh a-IGZO TFT devices. (b) The comparison of XPS O1s spectrum for the a-IGZO films with the furnace annealing at 450 °C for 1 h (upper side) and the microwave annealing at 2P for 100 s (lower side).

annealing at 450 °C for 1 h for comparison. The O1s peak of a-IGZO film with microwave annealing composed of a higher intensity of peak A and a lower intensity of peak B than those of the 450 °C furnace-annealed one. These material analysis results were consistent with the electrical improvement in device performance and reliability of a-IGZO TFT, since microwave annealing facilitated the formation of lattice oxygen and eliminated the defects originating from oxygen deficiency. Energy transfer to the a-IGZO TFT was even more effective by the microwave annealing process than that of the conventional furnace annealing.

In summary, this work has demonstrated the feasibility of high performance and reliable a-IGZO TFTs with microwave annealing process. Microwave annealing with low thermal budget can reduce the manufacturing process period and improve electrical characteristics of a-IGZO TFTs, due to the effective absorption of microwave energy by the a-IGZO active layer. This selective heating also potentially avoided the damage to materials neighboring the a-IGZO channel layer in the TFT device structure during thermal processes. With optimum microwave annealing around 1200 W for 100 s in this work, electrical performance and reliability of a-IGZO TFT are more significantly promoted than with furnace annealing at 450 °C for 1 h. Results of this study significantly contribute to microwave annealing applications for us in emerging flat-panel displays of transparent oxide TFTs technology.

The authors would like to thank the National Science Council of the Republic of China, Taiwan for financially supporting this research under Contract No. NSC 100-2628-E-009-016-MY3. National Nano Device Laboratories (Hsinchu, Taiwan) was commended for the use of its facilities.

[1]K. Nomura, H. Ohta, A. Takagi, T. Kamiya, M. Hirano, and H. Hosono, Nature **432**, 488 (2004).

[2]J. S. Park, K. S. Kim, Y. G. Park, and Y. G. Mo, Adv. Mater. **21**, 329 (2009).

[3]C. J. Chiu, S. P. Chang, and S. J. Chang, IEEE Electron Device Lett. **31**, 1245 (2010).

[4]P. T. Liu, Y. T. Chou, L. F. Teng, and C. S. Fuh, Appl. Phys. Lett. **97**, 083505 (2010).

This article is copyrighted as indicated in the article. Reuse of AIP content is subject to the terms at: http://scitation.aip.org/termsconditions. Downloaded to IP: 140.113.38.11 On: Thu, 01 May 2014 08:31:59

[5]P. T. Liu, Y. T. Chou, L. F. Teng, F. H. Li, and H. P. Shieh, Appl. Phys. Lett. **98**, 052102 (2011).
[6]K. Nomura, T. Kamiya, H. Ohta, M. Hirano, and H. Hosono, Appl. Phys. Lett. **93**, 192107 (2008).
[7]K. Nomura, T. Kamiya, Y. Kikuchi, M. Hirano, and H. Hosono, Thin Solid Films **518**, 3012 (2010).
[8]C. S. Fuh, S. M. Sze, P. T. Liu, L. F. Teng, and Y. T. Chou, Thin Solid Films **520**, 1489 (2011).
[9]J. R. Groza, S. H. Risbud, and K. Yamazaki, J. Mater. Res. **7**, 2643 (1992).
[10]T. F. Schulze, H. N. Beushausen, T. Hansmann, L. Korte, and B. Rech, Appl. Phys. Lett. **95**, 182108 (2009).
[11]H. L. Hortensius, A. Öztürk, P. Zeng, E. F. C. Driessen, and T. M. Klapwijk, Appl. Phys. Lett. **100**, 223112 (2012).
[12]Y. J. Lee, F. K. Hsueh, S. C. Huang, J. M. Kowalski, J. E. Kowalski, A. T. Y. Cheng, A. Koo, G. L. Luo, and C. Y. Wu, IEEE Electron Device Lett. **30**, 123 (2009).
[13]Y. J. Chen, M. S. Cao, T. H. Wang, and Q. Wan, Appl. Phys. Lett. **84**, 3367 (2004).
[14]R. F. Zhuo, L. Qiao, H. T. Feng, J. T. Chen, D. Yan, Z. G. Wu, and P. X. Yan, J. Appl. Phys. **104**, 094101 (2008).
[15]S. Y. Han, G. S. Herman, and C. H. Chang, J. Am. Chem. Soc. **133**, 5166 (2011).
[16]H. Cho, E. A. Douglas, A. Scheurmann, B. P. Gila, V. Craciun, E. S. Lamber, E. S. Pearton, and F. Ren, Electrochem. Solid-State Lett. **14**, H431 (2011).
[17]T. Jun, K. Song, Y. Jeong, K. Woo, D. Kim, C. Bae, and J. Moon, J. Mater. Chem. **21**, 1102 (2011).

This article is copyrighted as indicated in the article. Reuse of AIP content is subject to the terms at: http://scitation.aip.org/termsconditions. Downloaded to IP: 140.113.38.11 On: Thu, 01 May 2014 08:31:59